The Generation of Simulated Mammograms from Contrast Enhanced MRI for Surgical Planning and Postoperative Assessment

Christian P. Behrenbruch[1], Kostas Marias[1,2], Paul A. Armitage[1], J. Michael Brady[1], Jane Clarke[3], Niall Moore[4]

[1]Medical Vision Laboratory (Robotics), Oxford University, Parks Rd, Oxford OX1 3PJ, United Kingdom: {cpb,jmb}@robots.ox.ac.uk

[2]Department of Surgery, Royal Free and University College Medical School, UCL, London NW3 2QG, UK

[3]Department of Surgery, Churchill Hospital, Oxford OX3 7LJ, UK

[4]Magnetic Resonance Imaging Centre, John Radcliffe Hospital, Headley Way, Oxford OX3 9DU, UK

1. Introduction

There are numerous reasons for attempting to relate mammograms to "functional" images, typified by contrast-enhanced breast MRI. These include:

(i) Complementary pathological indicators. For example, microcalcifications present in a mammogram may meaningfully correlate with an enhancing region in MRI.

(ii) Patients having a pre-operative MRI scan have often already had a mammogram and therefore there is the opportunity not only to provide the clinician with more specific information to support diagnosis but also to maintain diagnostic consistency.

(iii) Younger patients often have both an MRI scan and a mammogram due to the limited effectiveness of using mammography for assessing pre-menopausal women.

(iv) Post-operative tissue changes may be difficult to assess with mammography and are often better evaluated with MRI. This is largely due to the high x-ray attenuation of scar tissue.

The objective of the present study is to demonstrate the simulation of mammograms from contrast-enhanced MRI, and to compare the simulated results to actual mammograms. By projecting MRI voxel contrast-enhancement (pharmacokinetic) information (figure 1) in a similar geometric fashion to a cranio-caudal and/or medio-lateral oblique view, and registering the mammograms to the resulting projection, it is possible to compare the

functional structure of tissues with the high-resolution structure of X-rays. The registration of X-rays to the reference frame of MRI enables not only point correspondence between mammogram views, but also approximates correspondence with imaged tissue using MRI.

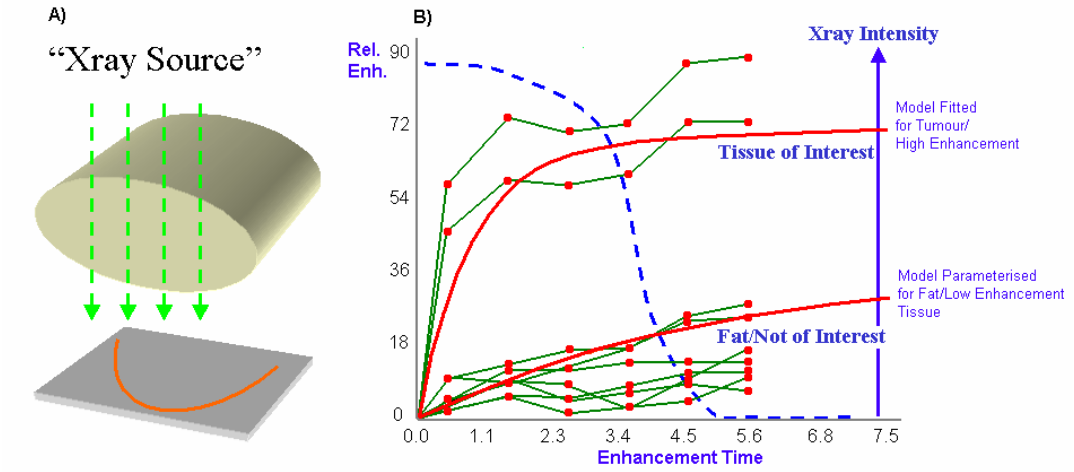

Figure 1. A) shows the conceptual geometry behind the projection process (for a cranio-caudal view), where the MRI voxel intensities are mapped into a transformed intensity plane. B) Shows some typical voxel enhancement graphs with the fitted pharmacokinetic model. The dashed line shows the effective result of integrating the fitted model to produce a projection intensity that is biased to voxels with high enhancement.

2. Projection Formation

The main idea behind this work is to create a projection of an MRI breast volume as an image that represents uncompressed tissue. However, rather than simply using an intensity-based projection or some kind of transfer function that maps MRI T1 values to approximate tissue X-ray attenuation characteristics (Gilhuijs 1995), we have chosen to project the actual voxel enhancement characteristics via a pharmacokinetic model (Kaiser, 1990, Hoffman et. al., 1995). The concept is illustrated in figure 1, where low enhancement tissues are given a low level of intensity in the "pseudo X-ray" projection. The projection intensity contribution of high-enhancement voxels are given a correspondingly high value. To map the projection intensities, we integrate the Hayton-Brady pharmacokinetic model of gadolinium uptake (Hayton et. al. 1997) for each voxel with respect to enhancement time. The main components of this model are depicted in figure 2.

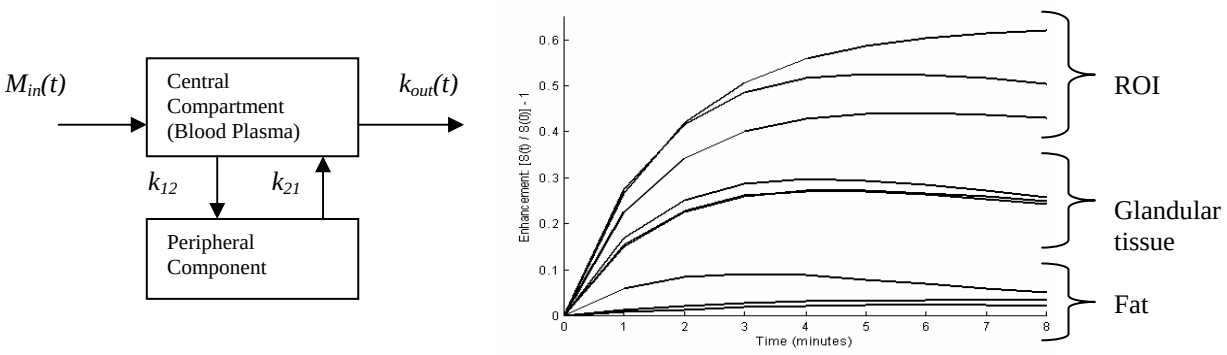

Figure 2. A two-compartment pharmacokinetic model with typical contrast curves for fat, parenchymal (glandular) tissue and enhancing regions of interest. M_{in} is the mass of contrast injected into the blood stream with respect to time. k_{12} and k_{21} are inter-compartment exchange rates and k_{out} is the leaving contrast rate.

Equation 1 shows the derived bolus model for gadolinium DTPA uptake which is fitted to the contrast data (via a Levenberg Marquart algorithm) to produce a difference of exponential parameterisation (see figure 2b for example curve fittings).

$$Concentrat\ ion(t) = \frac{A}{a-b}(\exp^{-bt} - \exp^{-at}) \qquad (1)$$

The parameters A,a and b characterise the exchange rates k_{12}, k_{21}, k_{in} *and* k_{out} (figure 2a) although for the purposes of controlling the projection, we are primarily interested in A and a (which approximately correspond to the maximum enhancement and the uptake rate of enhancement).

3. Projection Functional Characteristics

The result of the pharmacokinetic projection is a functional projection of the MRI volume that has a number of interesting characteristics. These are:

1. Fatty tissue receives almost no projection enhancement
2. Parenchymal (glandular) tissue is given an enhancement level that spatially corresponds well with the intensities that are observed in a mammogram image.
3. Rapidly-enhancing regions of interest (ROIs) are given extremely high relative contrast

These characteristics are demonstrated in the two cranio-caudal examples shown in figure 3. In the first pair, the patient has no pathology (except for a few coarse calcifications), however the glandular tissue is strongly pronounced in the mammogram due to ductal ectasia. These "exploded" ducts are clearly visible in the contrast-enhanced MRI projection as a correspondingly high level of contrast with respect to the fatty background. In the second example, the patient has a large, poorly differentiated tumour (outlined) that has a similar intensity to glandular tissue in the X-ray, but clearly stands out as a strongly enhancing region in the MRI projection. It is worth noting that the comparative resolution between the projections is quite different due to two main factors, namely the spatial resolution of the MRI scan (particularly the number of slices) and the degree of involution in the breast.

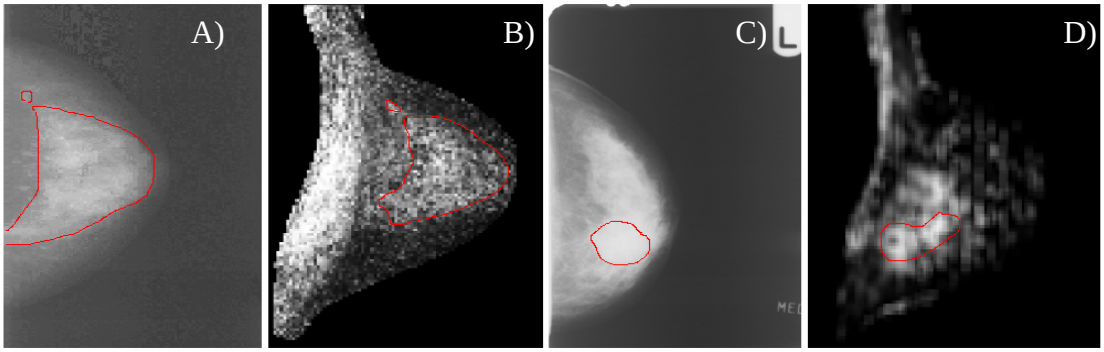

Figure 3: Two examples comparing the CC mammogram to corresponding contrast-enhanced MRI projections. The first example A), B) shows consistent shape characteristics of moderately-enhancing parenchymal tissue, due to ductal ectasia. The second pair C), D) compares the contrast of a large tumour in the X-ray image with the corresponding functional projection.

4. Alternative Pharmacokinetic Approaches

Recently, we have considered alternative pharmacokinetic models. The most simplistic of these is a statistical comparison of the integral of voxel enhancement. Although this provides reasonable tissue differentiation, the lack of a physiologically meaningful model to constrain the analysis renders the model highly susceptible to noise, particularly for low-enhancing fatty regions.

The model that has, to date, provided the best results is the Hayton-Brady model. As mentioned previously, this is a two-compartment exchange model. More complex models exist that include additional exchange components, notably that proposed by Tofts (Tofts & Kermote, 1991). However despite the simplified nature of the model that we are currently verifying, the low temporal resolution of the enhancement acquisition (7-9 time points, approximately 1-minute intervals) does not support system identification with more complex model representation. Of course, improved temporal resolution of the MRI acquisition sequence would make more complex models more applicable. In fact, such sequences are already widely in use. However, current clinical judgement accords greater emphasis to spatial rather than temporal resolution. We do not perceive this to be a limitation in light of our choice of model. We are, however, continuing to develop the enhancement model.

5. Motion Correction and Registration

There are two additional issues that require consideration in order to accurately compare the mammograms to their corresponding MRI functional projections. The first is motion correction. In order to evaluate the voxel enhancement with respect to time, it is necessary to ensure that tissue motion is limited. Since, including pre-contrast agent acquisitions, the MRI imaging takes around 10 minutes, it is unrealistic to expect that the patient will remain completely motionless, especially as women are naturally tense when imaging begins. A number of research groups have developed approaches to this problem including techniques utilising optical flow (Hayton et. al., 1997) and tensor splines as a deformation framework (Rueckert et. al., 1999). We currently utilise the approach developed by Hayton, which uses mutual information as a voxel similarity measure to control an optical flow based segmentation.

The second issue, which is perhaps of more clinical interest, is registering the mammograms to the MRI projection. We have developed a technique based on curvature measures and wavelet landmark detection that utilises thin-plate splines to accurately register images. This technique has been reliably applied to register temporal mammograms (Marias et. al., 1999/2000) and to perform 2D/3D data fusion between mammography and contrast-enhanced MRI. We refer to (Behrenbruch et. al., 2000) for further detail of the process. The result of registration is a complex deformation of the mammograms to the spatial reference frame of the MRI volume (via the projection). More specifically, the registration process has the effect of "uncompressing" the mammogram to resemble the minimally-compressed prone MRI breast. This is illustrated in figure 4, where the cranio-caudal mammogram in the earlier example (figure 3a,b) is registered to the corresponding MRI functional projection.

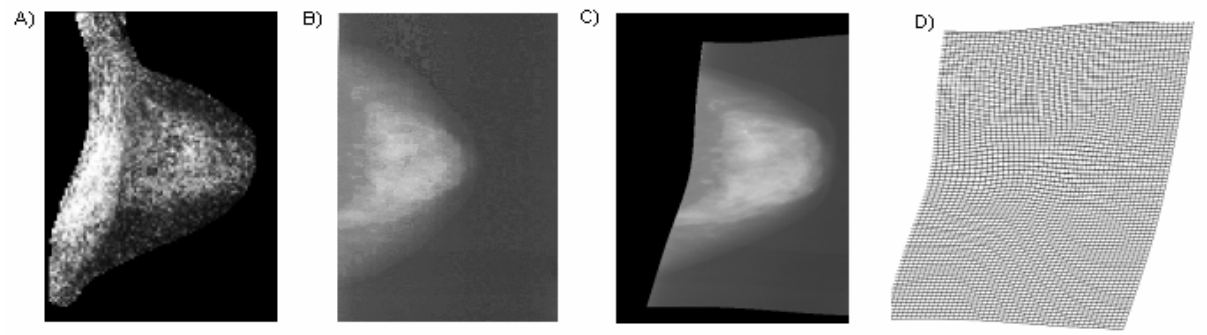

Figure 4. An example of registering a cranio-caudal mammogram A) to the corresponding MRI volume projection B). The resulting (cropped) deformation C) shows very good anatomical correspondence with the functional projection. D) shows the deformation of B) necessary to achieve the registration.

5. A Multimodal Approach to Pathology Assessment

Registration of the X-ray mammograms to the MRI projections enable three analyses:

- Point correspondence between the CC and MLO views.
- 3D point correspondence in the MRI volume with respect to features in the X-ray images.
- A projection-based comparison of functional information (from contrast enhanced MRI) with the detailed structural characteristics of the mammograms.

The first two applications of our technique are illustrated in Figure 5, where both the CC and MLO mammograms are registered to the MRI volume. In both X-ray views, two coarse calcifications are visible (highlighted). After registration, it is possible to correlate the positions of the calcifications between the two views, as well as to the position that the calcifications would have in the MRI volume. From a clinical perspective, this is interesting, since microcalcifications can not be studied using MRI and yet the additional pathological information provided by the mammogram potentially complements the enhancement characteristics of ductal carcinoma.

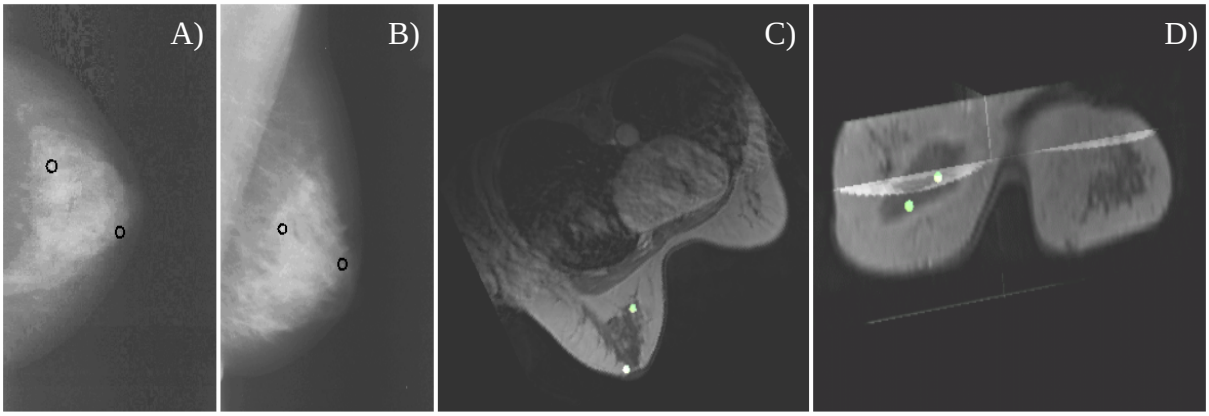

Figure 5. The cranio-caudal A) and lateral B) view showing the location of the two calcifications. C) and D) are 3D position reconstructions of the two calcifications within the MRI volume (volume resliced for clarity)

The third use of the functional projection technique involves comparison between the functional distribution of a pathology and the corresponding mammogram structure. There are many potential clinical applications for such comparisons, including pathology assessment and chemotherapy treatment evaluation. Additionally, pre-operative mammograms could be registered to a post-operative contrast-enhanced MRI scan to assess the success of an excision. This is useful in practice, since post-operative scarring tends to mask remaining pathology in a mammogram. However, since scar tissue has a relatively low level of contrast enhancement, a registered MRI projection would circumvent this difficulty.

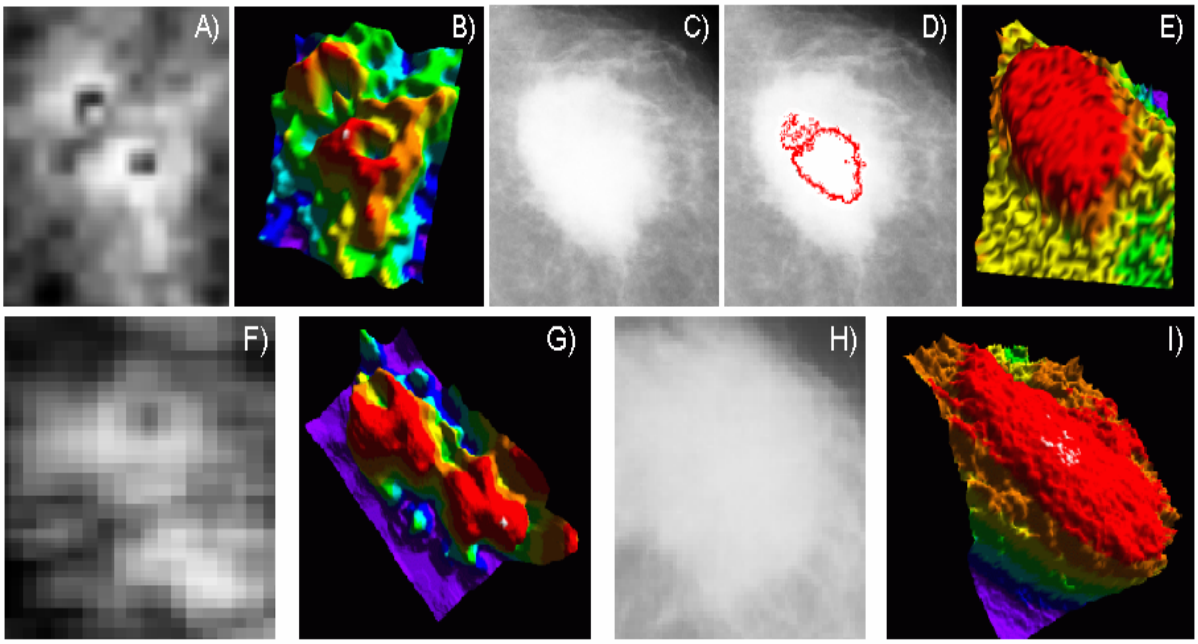

Figure 6. This figure shows two examples of large carcinomas that are poorly differentiated in the mammogram images (C, H). The corresponding registered MRI functional projections (A, F) provide additional information about vascularity and necrosis (visible as low-enhancement focal points). B) and G) show surface representations of the MRI projections to be compared with E) and I) which are the corresponding surface representations of tumours in the X-ray images. The first case is particularly interesting as the two necrotic regions can actually be correlated with structural information in the mammogram via some simple thresholding and edge detection D).

For the purpose of demonstrating a comparison between the functional information projected from the MRI volume and the pathology represented in the mammogram, figure 6 shows two examples of large, poorly differentiated tumours. Although they are clearly apparent in the mammograms, the additional functional information from the MRI is quite illuminating. The tumours appear are quite fibrous and spiculated, which consequently masks the necrosis. In the MRI projections, the vascular and necrotic components are well defined – particularly the necrosis which typically appears as comparatively low enhancement nucleus.

6. Discussion & Conclusion

To date, our technique has been applied to 12 sets of patient data with good results. We have assessed the performance of the functional projection approach on a wide range of

pathologies with very different structural and biomechanical properties. The technique has shown to be particularly effective in providing additional information about pathology vascularity and necrosis. The ability to correlate features in mammograms with enhancing regions in contrast-enhanced MRI is also potentially very useful, especially for studying the 3D distribution of microcalcification structures and correlating calcifications to the enhancement characteristics of ductal carcinoma in-situ (DCIS). Further work will focus on clinical validation with a larger data set (approximately 35 cases) as well as phantoms and core-biopsy studies. We also hope to use our technique as a data fusion framework for validating the h_int representation developed by Highnam and Brady (1999).

7. Acknowledgements

C. Behrenbruch would like to acknowledge the Commonwealth Scholarship and Fellowship Program for his doctoral funding at Oxford University. J.M. Brady acknowledges EPSRC support for his senior fellowship.

8. References

Behrenbruch, C.P., Marias, K., Yam, M., Brady, J. M., English, R. E., "The use of Magnetic Resonance Imaging to Model Breast Compression in X-ray Mammography for MR/X-ray Data Fusion", *Medical Physics, IWDM (International Workshop in Digital Mammography) 2000*, Toronto, Canada, June 2000.

Gilhuijs K.G.A., "Automated verification of radiation treatment geometry", Universiteit van Amsterdam, *Febo-druk*, Enschede-Utrecht, The Netherlands, 1995

Hayton, P., Brady, J.M., Tarassenko, L., Moore, N., "Analysis of dynamic MR breast images using a model of contrast enhancement", *Medical Image Analysis*, 1:3, April, 1997, Oxford University Press

Hoffman, U., Brix, G., Knopp, M.V., Hess , T., Lorentz. , W.J., "Pharmacokinetic mapping of the breast: A new method for dynamic MR mammography", *Magnetic Resonance in Medicine* 33, pp 506-514, 1995

Highnam, R.P., Brady, J.M., "Mammographic Image Processing", *Kluwer Academic Press*, 1999

Marias, K., Brady, J.M, Parbhoo, S., Seifalian, A.M., “Registration and matching of temporal mammograms for detecting abnormalities”, *Medical Imaging Understanding and Analysis*, Oxford 1999

Kaiser, W.A., “Dynamic magnetic resonance breast imaging using a double breast coil: an important step towards routine examination of the breast”, *Frontiers in European Radiology* 7, pp 39-68, 1990

Marias, K., Behrenbruch, C.P., Brady, J.M., Parbhoo, S., Seifalian, “Multi-scale Landmark Selection for Improved Registration of Temporal Mammograms”, *IWDM (International Workshop in Digital Mammography) 2000*, Toronto, Canada, Elsevier, June 2000

Rueckert, D., Sonoda, L.I., Denton, E., Rankin, S., Hayes, C., Leach, M.O., Hill, D., Hawkes, D.J., “Evaluation of Non-rigid Registration using Free-Form Deformation for Breast MR Images, Medical Image Understanding and Analysis, Oxford, July 1999

Tofts, P. A. Kermode, A., “Measurement of the blood-brain barrier and leakage space using dynamic MR imaging 1. Fundamental concepts”, *Magnetic Resonance in Medicine* **17**, pp 347-367, 1991